Robotica (2010) volume 28, pp. 1065–1072. © Cambridge University Press 2010
doi:10.1017/S0263574709990555

Design and kinematics analysis of a new 3CCC parallel mechanism

Dongming Gan†,‡,*, Qizheng Liao†, Jian S. Dai‡ and Shimin Wei†

†*Beijing University of Posts and Telecommunications, Beijing 100876, China*
‡*King's College London, University of London, Strand, London WC2R2LS, UK*

(Received in Final Form: September 11, 2009. First published online: February 10, 2010)

SUMMARY
A CCC limb and a new 3CCC parallel mechanism have been designed in this paper based on geometry analysis. Their mobility and geometrical constraints are discussed by using screw theory and geometrical equations separately. Following that both the inverse and forward kinematics of the 3CCC parallel mechanism are proposed, in which Dixon's resultant is used to get the forward solutions for the orientation and a eighth-order polynomial equation in one unknown is obtained, leading to the results for the position analysis, numerical examples confirm these theoretical results. A short comparison with the traditional Stewart platforms is presented in terms of kinematics, workspace and trajectory planning.

KEYWORDS: General Stewart platform; Cylinder; Kinematics; Mobility; Workspace.

1. Introduction

The studies of parallel mechanisms started with the conception of the general 6–6 Stewart–Gough structure, proposed by Gough[1] with a tire testing machine and Stewart[2] with a flight simulator. Compared to serial mechanisms, parallel mechanisms provide increased stiffness, resulting in improved positional accuracy and strength. For the past several decades, the Stewart–Gough platform and its variants[3–6] have been widely studied, including their accuracy,[7] workspace,[8] stiffness,[9] etc. Generally, the Stewart–Gough platform consists of a moving platform, a fixed base and six SPS (spherical joint, prismatic joint, spherical joint) limbs and has mobility six.

One of the most important issues of a parallel mechanism study is the kinematics analysis, generating results that form the base for the application of the mechanism. The forward kinematics problem, finding the position and orientation of the moving platform given the actuator displacements, is analytically complex, while the inverse positional problem is much easier and the former usually leads naturally to a system of highly nonlinear algebraic equations with multiple solutions, which has been proved a very difficult task. Angeles *et al.*[10] gave the real-time direct kinematics of general six degree of freedom (DOF) parallel manipulators by using sensors. For the first time, Husty[11] produced a 40th-degree univariate equation for the general 6–6 Stewart platform by finding the greatest common divisor of the intermediate polynomials of degree 320. Lee and Shim[12] developed an elimination method to solve the forward kinematics of the general 6–6 Stewart platform by deriving directly a univariate polynomial of degree 40 from a 15×15 matrix while Merlet[13] proposed an efficient algorithm to deal with the same type 6-DOF parallel mechanism based on interval analysis.

The difficulty in solving the direct kinematics problem is considered to be a major obstacle of using the Stewart–Gough platform in many applications. From this point of view, Chinese mathematician Gao Xiaoshan[14] introduced the generalized Stewart–Gough platform (GSP), which could be considered as the most general form of parallel manipulators with 6-DOF in certain sense. A GSP consists of two rigid bodies connected with six distance or/and angular constraints between six pairs of points, lines and/or planes in the base and platform respectively. The traditional parallel platforms are all special cases of the GSPs. Some of these new GSPs can provide new parallel manipulators which have the stiffness and lightness of the Stewart–Gough platform and easy to solve direct kinematics.

Presented in this paper is the solution to a new 3CCC parallel mechanism, which is one of the 3A3D GSPs that have three angular and three distance constraints. Figure 1 shows a special case of the 3CCC parallel mechanism. This new mechanism consists of cylindrical joints only, which are better on stiffness than the traditional spherical joints. The constraints of the 3-CCC are between three pairs of lines in the base and platform, respectively. It is shown that the position and orientation of the platform are decoupled and the forward solutions of them are both eighth-order polynomial equations. The equations are numerically solved, and two numerical examples are given to confirm these theoretical results.

2. Design of the CCC limb, the 3CCC Parallel Mechanism and Its Mobility Analysis

2.1. Design of the CCC limb

Geometrically, the traditional SPS limb supports the platform in variable configurations by changing the distance constraint between the two spherical centres at the two ends as in Fig. 2. Based on the study in ref. [14], the constraint can be a distance

* Corresponding author. E-mail: gandong64@sina.com

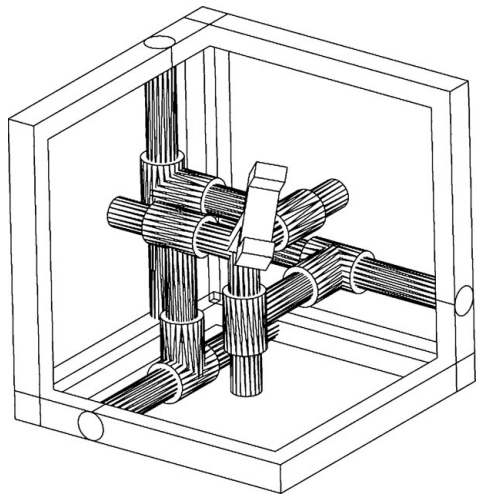

Fig. 1. A special 3CCC parallel mechanism.

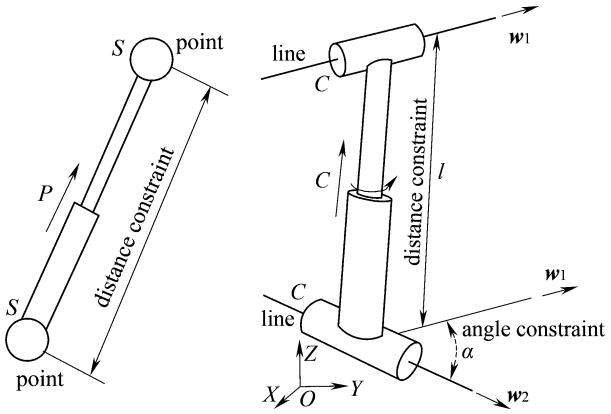

Fig. 2. The SPS limb and CCC limb.

between any two of a point, a line and a plane and can be an angle between two lines or a line and a plane. The general SPS can be taken as that has a distance constraint between two points. Using this theory, we construct a new limb that has both distance and angle constraints as in Fig. 2, which consists of three cylindrical joints with two on the base and platform separately and another one along the limb.

As in Fig. 2, set a fixed frame *OXYZ*, w_1 and w_2 denote the unit vectors of the two cylindrical joints at the two ends, expressed in *OXYZ*. The distance and angle constraints of the limb will be the distance and angle between w_1 and w_2, denoted as l and α separately, and can be operated by changing the distance of and rotating the cylindrical joint along the limb. In *OXYZ*, the constraint equations can be given as

angle constraint:

$$\cos(\alpha) = \boldsymbol{w}_1^T \boldsymbol{w}_2, \tag{1}$$

distance constraint:

$$l^2(\boldsymbol{w}_1 \times \boldsymbol{w}_2) \cdot (\boldsymbol{w}_1 \times \boldsymbol{w}_2) = ((\boldsymbol{b} - \boldsymbol{a}) \cdot (\boldsymbol{w}_1 \times \boldsymbol{w}_2))^2, \tag{2}$$

where $\boldsymbol{a}$ and $\boldsymbol{b}$ are vectors of two arbitrary points on $\boldsymbol{w}_1$ and $\boldsymbol{w}_2$ separately in *OXYZ*.

As the two-end cylindrical joints are perpendicular to the limb, $\boldsymbol{w}_1$ and $\boldsymbol{w}_2$ are in parallel planes. $\alpha(-\pi, \pi)$ is under the right-hand rule: holding the limb between $\boldsymbol{w}_1$ and $\boldsymbol{w}_2$ with the thumb of the right hand pointing to $\boldsymbol{w}_1$, rotating the other four fingers from $\boldsymbol{w}_1$ to $\boldsymbol{w}_2$, if α is the same side it is plus, otherwise it is minus. When $\boldsymbol{w}_1$ and $\boldsymbol{w}_2$ are parallel, $a = 0$ and Eq. (2) will be identically equal, thus this case should be avoided.

2.2. Design of the 3CCC parallel mechanism and Its mobility analysis

The 3-CCC parallel platform is shown in Fig. 3. There are three cylindrical limbs which are connected to the three cylindrical joints in the moving platform and to the three cylindrical joints in the base. In general case, the shapes of both moving platform and base are arbitrarily chosen in three-dimensional space which means for both moving and fixed platform, the cylindrical joints are not restricted to lie in a plane or intersect at one point. Thus Fig. 1 shows a special

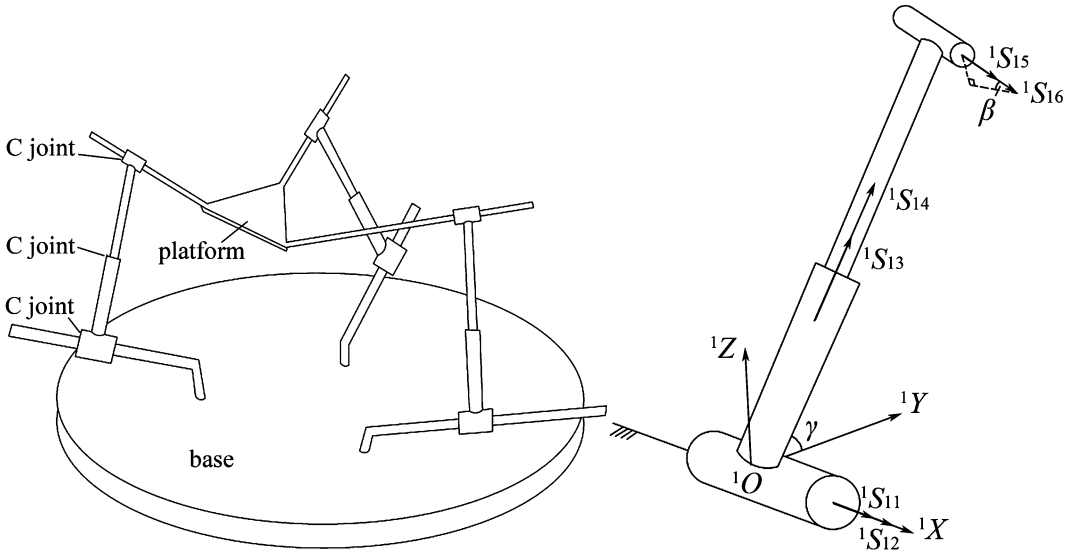

Fig. 3. A 3CCC parallel mechanism and the CCC limb.

https://doi.org/10.1017/S0263574709990555 Published online by Cambridge University Press

3CCC parallel mechanism with the three cylindrical joints perpendicular and intersecting each other on the platform.

As all the limbs of the 3CCC parallel mechanism have the same structure by analysing one of them in a common configuration and expanding the result to others, the constraints to the moving platform can be obtained and the mobility of the whole mechanism is known. Figure 3 shows a CCC limb in the general case. Using a local coordinate system ${}^1O{}^1X{}^1Y{}^1Z$ at the centre of the lower cylindrical joint with ${}^1X$-axis along the same line with the cylindrical joint and ${}^1Z$-axis perpendicular to the base plane, the limb twist system can be obtained as

$$\{{}^1\boldsymbol{S}_1\} = \begin{Bmatrix} {}^1\boldsymbol{S}_{11} = [1 \quad 0 \quad 0 \quad 0 \quad 0 \quad 0] \\ {}^1\boldsymbol{S}_{12} = [0 \quad 0 \quad 0 \quad 1 \quad 0 \quad 0] \\ {}^1\boldsymbol{S}_{13} = [0 \quad \cos\gamma \quad \sin\gamma \quad 0 \quad 0 \quad 0] \\ {}^1\boldsymbol{S}_{14} = [0 \quad 0 \quad 0 \quad 0 \quad \cos\gamma \quad \sin\gamma] \\ {}^1\boldsymbol{S}_{15} = [\cos\beta \quad \sin\alpha\sin\beta \quad -\cos\alpha\sin\beta \\ \qquad -l\sin\beta \quad l\cos\beta\sin\gamma \quad -l\cos\beta\cos\gamma] \\ {}^1\boldsymbol{S}_{16}\, x = [0 \quad 0 \quad 0 \quad \cos\beta \quad \sin\alpha\sin\beta \quad -\cos\alpha\sin\beta] \end{Bmatrix} \tag{3}$$

where the first two are for the lower C joint, the third and forth are for the middle C joint and the last two are for the upper C joint, γ is the angle between ${}^1\boldsymbol{S}_{13}$ and ${}^1Y$, β is the angle between ${}^1\boldsymbol{S}_{15}$ and its projection on ${}^1Y{}^1O{}^1Z$ plane, l is the distance between the centres of the upper and lower cylindrical joint in the limb.

Calculating the reciprocal screws to Eq. (3), the limb constraint system can be obtained as

$$\left\{{}^1\boldsymbol{S}_1^r\right\} = {}^1\boldsymbol{S}_{11}^r = [0 \quad 0 \quad 0 \quad 0 \quad 0 \quad 0]. \tag{4}$$

Thus the six twists in Eq. (3) form a six-system,[15] and there is no constraint to the platform with this kind of CCC limb, there are also no local degrees of freedom within the limb as there is no redundant twist in Eq. (3).

Thus the 3CCC parallel mechanism should have six degrees of freedom in the three-dimensional space as all the three CCC limbs do not supply any constraints to the moving platform. A distance actuator and an angular actuator can be attached to each CCC limb. The lengths of three limbs (l_1, l_2, l_3) and the angles (α_1, α_2, α_3) between three pairs of cylindrical lines are the inputs. The system outputs are the position and orientation of the moving platform.

3. Kinematics Analysis

3.1. Inverse kinematics

Figure 4 shows the kinematics model of the 3CCC parallel mechanism. Locate a fixed frame $OXYZ$ on the base and attach a moving frame $O'X'Y'Z'$ to the upper platform. ($\boldsymbol{v}_1$, $\boldsymbol{v}_2$, $\boldsymbol{v}_3$) and ($\boldsymbol{u}_1$, $\boldsymbol{u}_2$, $\boldsymbol{u}_3$) are the unit orientation vectors of the cylindrical joints on the platform and base, separately described in the moving frame and fixed frame. Let $\boldsymbol{a}_i$ denote the vector expressed in the fixed frame from the origin of the moving frame to an arbitrary point A_i on the line $\boldsymbol{u}_i$, $\boldsymbol{b}_i$ denote the vector from the origin of the moving frame to an arbitrary point B_i on the line $\boldsymbol{v}_i$. $\boldsymbol{P}$ denotes the vector

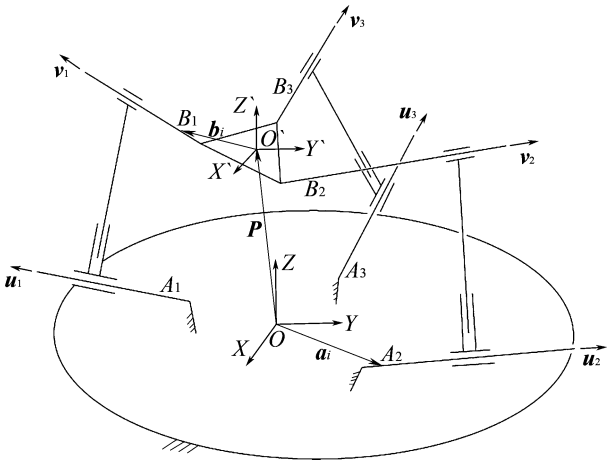

Fig. 4. Kinematics model of the 3CCC parallel mechanism.

from O to O' expressed in the fixed frame, l_i denotes the ith limb length, $\alpha_i(-\pi, \pi)$ denotes the angle between the two cylindrical joints $\boldsymbol{v}_i$ and $\boldsymbol{u}_i$. $\mathbf{R}$ is the 3×3 rotational matrix denoting the orientation of the moving frame with respect to the fixed frame. When the lengths of three limbs (l_1, l_2, l_3) and the angles (α_1, α_2, α_3) between three pairs of cylindrical lines are given, the corresponding constraint equations of the 3CCC parallel mechanism are as follows:

angle constraints:

$$\cos(\alpha_i) = (\mathbf{R}\mathbf{v}_i)^T\mathbf{u}_i \quad (i = 1, 2, 3), \tag{5}$$

distance constraints:

$$l_i^2(\boldsymbol{R}\boldsymbol{v}_i \times \boldsymbol{u}_i)\cdot(\boldsymbol{R}\boldsymbol{v}_i \times \boldsymbol{u}_i) = ((\boldsymbol{R}\boldsymbol{b}_i + \boldsymbol{P} - \boldsymbol{a}_i)\cdot(\boldsymbol{R}\boldsymbol{v}_i \times \boldsymbol{u}_i))^2 \quad (i = 1, 2, 3). \tag{6}$$

The problem of inverse kinematics is that orientation $\boldsymbol{R}$ and position $\boldsymbol{P}$ of the platform are known to solve the actuation of the limbs. Thus from Eqs. (5) and (6), the actuation (l_1, l_2, l_3, α_1, α_2, α_3) of the three limbs can be solved directly as

$$\alpha_i = \mathrm{ArcCos}((\boldsymbol{R}\boldsymbol{v}_i)^T\boldsymbol{u}_i), \quad (i = 1, 2, 3), \tag{7}$$

$$l_i = \sqrt{((\boldsymbol{R}\boldsymbol{b}_i + \boldsymbol{P} - \boldsymbol{a}_i)\cdot(\boldsymbol{R}\boldsymbol{v}_i \times \boldsymbol{u}_i))^2/(\boldsymbol{R}\boldsymbol{v}_i \times \boldsymbol{u}_i)\cdot(\boldsymbol{R}\boldsymbol{v}_i \times \boldsymbol{u}_i)}, \quad (i = 1, 2, 3). \tag{8}$$

3.2. Forward kinematics

From Fig. 4, without loss of generality, assume that

$$\left.\begin{aligned} \boldsymbol{P} &= (x, y, z)^T, \\ \boldsymbol{u}_i &= (u_{i1}, u_{i2}, u_{i3})^T, \\ \boldsymbol{v}_i &= (v_{i1}, v_{i2}, v_{i3})^T, \\ \boldsymbol{a}_i &= (a_{i1}, a_{i2}, a_{i3})^T, \\ \boldsymbol{b}_i &= (b_{i1}, b_{i2}, b_{i3})^T, \\ &(i = 1, 2, 3). \end{aligned}\right\} \tag{9}$$

In the three-dimensional coordinate system, a rigid body rotates an angle θ about an axis $\boldsymbol{K}$ (kx, ky, kz), the rotation

https://doi.org/10.1017/S0263574709990555 Published online by Cambridge University Press

matrix $\boldsymbol{R}$ can be given as follows:[16]

$$\boldsymbol{R}_k(\theta)=\begin{bmatrix} k_x^2 v\theta + c\theta & k_x k_y v\theta - k_z s\theta & k_x k_z v\theta + k_y s\theta \\ k_x k_y v\theta + k_z s\theta & k_y^2 v\theta + c\theta & k_y k_z v\theta - k_x s\theta \\ k_x k_z v\theta - k_y s\theta & k_y k_z v\theta + k_x s\theta & k_z^2 v\theta + c\theta \end{bmatrix}, \tag{10}$$

where $c\theta = \cos\theta$, $s\theta = \sin\theta$, $v\theta = 1 - \cos\theta$

Set:

$$\left.\begin{aligned} &c_1 = k_x \tan(\theta/2), \\ &c_2 = k_y \tan(\theta/2), \\ &c_3 = k_z \tan(\theta/2), \\ &\cos(\theta) = (1 - \tan^2(\theta/2))/(1 + \tan^2(\theta/2)), \\ &\sin(\theta) = 2\tan(\theta/2)/(1 + \tan^2(\theta/2)), \end{aligned}\right\} \tag{11}$$

where c_1, c_2 and c_3 are the Rodriguez–Hamilton parameters. As usually θ is less than π, (11) can avoid the singularity and be used in following procedure.

Substituting Eq. (11) into (10) yields

$$\boldsymbol{R} = \Delta^{-1}\begin{bmatrix} 1 + c_1^2 - c_2^2 - c_3^2 & 2(c_1c_2 - c_3) & 2(c_1c_3 + c_2) \\ 2(c_1c_2 + c_3) & 1 - c_1^2 + c_2^2 - c_3^2 & 2(c_2c_3 - c_1) \\ 2(c_1c_3 - c_2) & 2(c_2c_3 + c_1) & 1 - c_1^2 - c_2^2 + c_3^2 \end{bmatrix}, \tag{12}$$

where $\Delta = 1 + c_1^2 + c_2^2 + c_3^2$, (12) is the *Cayley*[17] formula.

Substituting Eqs. (9) and (12) into Eqs. (5) and (6), simplifying and taking the numerator, we have

$$Eq_e(c_1, c_2, c_3) = \sum_{\substack{i,j,k=0 \\ i+j+k\le 2}}^{2} g_{e-ijk} c_1^i c_2^j c_3^k = 0, \quad (e = 0, 1, 2), \tag{13}$$

$$(zr_{i1} + yr_{i2} + xr_{i3})^2 - l_i^2 r_{i4} = 0, \quad (i = 1, 2, 3), \tag{14}$$

where g_{e-ijk} are real constants depending on input data only, r_{ij} are functions in c_1, c_2, c_3 and other input data.

The forward displacement analysis of the 3CCC parallel mechanism can be described as: solve the six unknown (x, y, z, c_1, c_2, c_3) when the three lengths l_i and the three angles α_i are given with the six equations in Eqs. (13) and (14). Observing Eqs. (13) and (14), it can be found that that the position and orientation of the moving platform of the 3CCC parallel mechanism are decoupled as Eq. (13) are three equations in c_1, c_2, c_3 only. Thus the procedure of solving the forward displacement problem can be: First, solving c_1, c_2, c_3 using Eq. (13) and giving the results of orientation $\boldsymbol{R}$; second, substituting results of c_1, c_2, c_3 into Eq. (14) to get corresponding results of position $\boldsymbol{P}$.

3.2.1. Solving the orientation $\boldsymbol{R}$: (1) Solutions of c_3 rewrite Eq. (13) as the function of c_1, c_2 by putting the products of power in c_3 into the coefficients

$$Q_e(c_1, c_2) = \sum_{\substack{i,j=0 \\ i+j\le 2}}^{2} G_{e-ij} c_1^i c_2^j = 0, \quad (e = 0, 1, 2), \tag{15}$$

where G_{e-ij} are function of g_{e-ijk} and the products of power in c_3

According to Dixon's resultant principle,[18,19] a 3×3 matrix $\boldsymbol{D}$ can be obtained using Eq. (15) after executing the following algorithm:

Construct the following matrix

$$\Delta(c_1, c_2, t_1, t_2) = \begin{vmatrix} Q_0(c_1, c_2) & Q_1(c_1, c_2) & Q_2(c_1, c_2) \\ Q_0(t_1, c_2) & Q_1(t_1, c_2) & Q_2(t_1, c_2) \\ Q_0(t_1, t_2) & Q_1(t_1, t_2) & Q_2(t_1, t_2) \end{vmatrix}, \tag{16}$$

where t_1, t_2 are intermediate parameters only. By developing the above equation, $\Delta(c_1, c_2, t_1, t_2)$ is a polynomial of degree 2 in c_1, 3 in c_2, 3 in t_1, 2 in t_2. Dixon observed that Δ vanishes when t_1, t_2 substitute for c_1, c_2, implying that $(c_1 - t_1)$(c_2 - t_2) is a factor of Δ. Therefore, the expression

$$\delta(c_1, c_2, t_1, t_2) = \frac{\Delta(c_1, c_2, t_1, t_2)}{(c_1 - t_1)(c_2 - t_2)} = 0 \tag{17}$$

is a polynomial of degree 1 in c_1, 2 in c_2, 2 in t_1, 1 in t_2. δ vanishes when $Q_0(c_1, c_2)$, $Q_1(c_1, c_2)$ and $Q_2(c_1, c_2)$ have common zeros no matter what t_1, t_2 are. The coefficients of each power product $t_1^i t_2^j (i = 0, 1, 2; j = 0, 1)$ of δ have common zeros which are also the common zeros of equations Q_0, Q_1, Q_2. This gives five equations in power product of c_1 and c_2, whereas the number of the power product $c_1^i c_2^j (i = 0, 1; j = 0, 1, 2)$ is also five. Therefore, the coefficients of each power product $c_1^i c_2^j$ in these five equations form a 5×5 matrix $\boldsymbol{D}$. All the above algorithm can be expressed as

$$\delta(c_1, c_2, t_1, t_2) = \frac{\Delta(c_1, c_2, t_1, t_2)}{(c_1 - t_1)(c_2 - t_2)} = \boldsymbol{T} \bullet \boldsymbol{D} \bullet \boldsymbol{C}^T = 0, \tag{18}$$

where $\mathbf{T} = [1 \;\; t_1 \;\; t_1^2 \;\; t_2 \;\; t_1 t_2]$, $\mathbf{C} = [1 \;\; c_2 \;\; c_2^2 \;\; c_1 \;\; c_2 c_1]$ and $\boldsymbol{D}$ is a matrix whose elements are polynomials in c_3.

Dixon also proved that Eq. (15) have common zeros if the determinant of the matrix $\boldsymbol{D}$ equals 0. Thus an equation in c_3 can be got:

$$\mathbf{det} = |\boldsymbol{D}| = 0, \tag{19}$$

where **det** is the determinant of matrix $\boldsymbol{D}$.

By expanding each elements of matrix $\boldsymbol{D}$, the degrees in c_3 can be shown as below:

$$\begin{bmatrix} 2 & 3 & 3 & 2 & 2 \\ 3 & 2 & 2 & 1 & 1 \\ 2 & 1 & 1 & 0 & 0 \\ 3 & 2 & 2 & 1 & 1 \\ 2 & 1 & 1 & 0 & 0 \end{bmatrix}. \tag{20}$$

https://doi.org/10.1017/S0263574709990555 Published online by Cambridge University Press

Therefore expanding Eq. (19) there is an equation of the highest degree $3+3+2+0=8$ in c_3:

$$\sum_{i=0}^{+8} h_i c_3^i = 0, \tag{21}$$

where h_i are real constants depending on input data only.

This implies that an univariate equation in c_3 of degree 8 is obtained.

(2) Solutions of c_1, c_2

Solving Eq. (21), all the solutions for c_3 can be obtained. Then substitute c_3 into the following equation:

$$\mathbf{D} \bullet \mathbf{C}^T = 0. \tag{22}$$

According to the Crame's rule, the solutions of c_1, c_2 can be computed from the above linear system.

Substituting all the solutions of c_1, c_2 and c_3 to Eq. (12), orientation $\mathbf{R}$ can be obtained.

3.2.2. An easy way to solve $\boldsymbol{R}$ *when* ($\boldsymbol{v}_1$, $\boldsymbol{v}_2$, $\boldsymbol{v}_3$) *are perpendicular to each other and intersect at one point*: In this case, the mechanism is as shown in Fig. 1. Thus the parameters can be set as $\boldsymbol{u}_1 = \boldsymbol{v}_1 = (1, 0, 0)$, $\boldsymbol{u}_2 = \boldsymbol{v}_2 = (0, 1, 0)$, $\boldsymbol{u}_3 = \boldsymbol{v}_3 = (0, 0, 1)$, $\boldsymbol{a}_1(0, a_1, 0)$, $\boldsymbol{a}_2(0, 0, a_2)$, $\boldsymbol{a}_3(a_3, 0, 0)$, $\boldsymbol{b}_i = (0, 0, 0)(i = 1, 2, 3)$, substituting them into Eq. (5) there are

$$\left.\begin{aligned} 1+(1-\cos\alpha_1)c_1^2-(1+\cos\alpha_1)c_2^2-(1+\cos\alpha_1)c_3^2=0,\\ 1-(1+\cos\alpha_2)c_1^2+(1-\cos\alpha_2)c_2^2-(1+\cos\alpha_2)c_3^2=0,\\ 1-(1+\cos\alpha_3)c_1^2-(1+\cos\alpha_3)c_2^2+(1-\cos\alpha_3)c_3^2=0. \end{aligned}\right\} \tag{23}$$

These are three linear equations in c_1^2, c_2^2, c_3^2, thus the results can be easily got as

$$\left.\begin{aligned} c_1 = \pm\sqrt{R_x/R_D},\\ c_2 = \pm\sqrt{R_y/R_D},\\ c_3 = \pm\sqrt{R_z/R_D}, \end{aligned}\right\} \tag{24}$$

where

$$\begin{aligned} R_x &= -2-2\cos\alpha_1+\cos\alpha_2+\cos\alpha_3,\\ R_y &= -2+\cos\alpha_1-2\cos\alpha_2+\cos\alpha_3,\\ R_z &= -2+\cos\alpha_1+\cos\alpha_2-2\cos\alpha_3,\\ R_D &= -2-2\cos\alpha_1-2\cos\alpha_2-2\cos\alpha_3. \end{aligned}$$

Any one of c_1, c_2 and c_3 has $+/-$ two solutions, so totally there are eight solution assemblies corresponding to eight orientations.

3.2.3. Solving position $\boldsymbol{P}$: Substitute solutions of c_1, c_2 and c_3 into Eq. (14), there are

$$n_i^2 - l_i^2 r_{i4} = 0, \quad (i = 1, 2, 3), \tag{25}$$

where

$$n_i = z r_{i1} + y r_{i2} + x r_{i3}, \quad (i = 1, 2, 3). \tag{26}$$

n_1, n_2 and n_3 can be solved from (25) directly as

$$n_i = \pm l_i \sqrt{r_{i4}}, \quad (i = 1, 2, 3). \tag{27}$$

Then substitute the solutions of n_1, n_2 and n_3 into (26), solutions of x, y and z can be obtained linearly using Crame's rule:

$$\left.\begin{aligned} x = D_x/D_D,\\ y = D_y/D_D,\\ z = D_z/D_D, \end{aligned}\right\} \tag{28}$$

where

$$\begin{aligned} D_x &= -r_{13}r_{22}n_3 + r_{12}r_{23}n_3 + r_{13}n_2r_{32} - n_1r_{23}r_{32}\\ &\quad -r_{12}n_2r_{33} + n_1r_{22}r_{33},\\ D_y &= -r_{13}n_2r_{31} + n_1r_{23}r_{31} + r_{13}r_{21}n_3 - r_{11}r_{23}n_3\\ &\quad -n_1r_{21}r_{33} + r_{11}n_2r_{33},\\ D_z &= -n_1r_{22}r_{31} + r_{12}n_2r_{31} + n_1r_{21}r_{32} - r_{11}n_2r_{32}\\ &\quad -r_{12}r_{21}n_3 + r_{11}r_{22}n_3,\\ D_D &= -r_{13}r_{22}r_{31} + r_{12}r_{23}r_{31} + r_{13}r_{21}r_{32} - r_{11}r_{23}r_{32}\\ &\quad -r_{12}r_{21}r_{33} + r_{11}r_{22}r_{33}. \end{aligned}$$

Thus there are eight solutions of n_i then eight solutions of position $\boldsymbol{P}(x, y, z)$ corresponding to one set of solutions of $\boldsymbol{R}$. So by giving the three distance and three angle inputs, there are $8 \times 8 = 64$ sets of solutions of the forward kinematics analysis of the 3CCC parallel mechanism, where the orientation and position are decoupled.

4. Numerical Verification for the Forward Kinematics

4.1. Example one

Parameters of a 3CCC parallel mechanism are given as $\boldsymbol{a}_1 = (0, 0, 0)$, $\boldsymbol{a}_2 = (0, 1.2, 2.07846)$, $\boldsymbol{a}_3 = (2, 2, 2.8)$, $\boldsymbol{b}_1 = (0, 0, 0)$, $\boldsymbol{b}_2 = (0.7, -0.7, 0)$, $\boldsymbol{b}_3 = (1, 1, -1.4)$, $\boldsymbol{u}_1 = (1, 0, 0)$, $\boldsymbol{u}_2 = (0, 1/2, \sqrt{3}/2)$, $\boldsymbol{u}_3 = (1/2, 1/2, \sqrt{2}/2)$, $\boldsymbol{v}_1 = (1, 0, 0)$, $\boldsymbol{v}_2 = (\sqrt{2}/2, -\sqrt{2}/2, 0)$, $\boldsymbol{v}_3 = (-1/2, -1/2, \sqrt{2}/2)$, $l_1 = 50$, $l_2 = 21.5124$, $l_3 = 37.0951$, $\alpha_1 = \mathrm{Arc}Cos(-1/2)$, $\alpha_2 = \mathrm{Arc}Cos(-0.12941)$, $\alpha_3 = \mathrm{Arc}Cos(-3/4)$. The solutions of the forward kinematics are obtained by using the procedure proposed above and listed in Table I. The results for this example containing 4 sets of real roots of the orientation with each has eight solutions for the position, corresponding to 32 moving platform configurations as two are shown in Fig. 5 (the middle cylindrical joint is shown in red with the base in blue and platform in green). All the roots have been checked by substituting in Eqs. (3) and (4). The validity of all of the roots shows that univariate equation and the whole process is correct.

4.2. Example two

Another example is analysed where ($\boldsymbol{v}_1$, $\boldsymbol{v}_2$, $\boldsymbol{v}_3$) are perpendicular to each other and intersect at one point, the parameters are $\boldsymbol{a}_1 = \boldsymbol{a}_2 = \boldsymbol{a}_3 = (0, 0, 0)$, $\boldsymbol{b}_1 = \boldsymbol{b}_2 = \boldsymbol{b}_3 = (0, 0, 0)$, $\boldsymbol{u}_1 = (1, 0, 0)$, $\boldsymbol{u}_2 = (0, 1, 0)$, $\boldsymbol{u}_3 = (0, 0, 1)$, $\boldsymbol{v}_1 =$

https://doi.org/10.1017/S0263574709990555 Published online by Cambridge University Press

Table I. Solutions of example one.

	Solutions of orientation				Solutions of position corresponding to root 3 of orientation		
	c_1	c_2	c_3		x	y	z
1	−4.07337	0.542502	7.2445	1	−172.169	−49.4996	−50
2	0.121002	0.689641	1.6026	2	172.169	49.4996	50
3	0.	0.	−1.73205	3	112.601	−24.1967	−50
4	−0.259–0.313i	1.373+0.324i	−1.100+0.151i	4	−112.601	24.1967	50
5	−0.259+0.313i	1.373–0.324i	−1.100–0.151i	5	17.4318	1.30371	−50
6	0.0997714	0.745702	−1.57283	6	−17.4318	−1.30371	50
7	0.088–0.977i	−0.461–0.376i	0.691–0.627i	7	−77	−75	−50
8	0.088+0.977i	−0.461+0.376i	0.691+0.627i	8	77	75	50

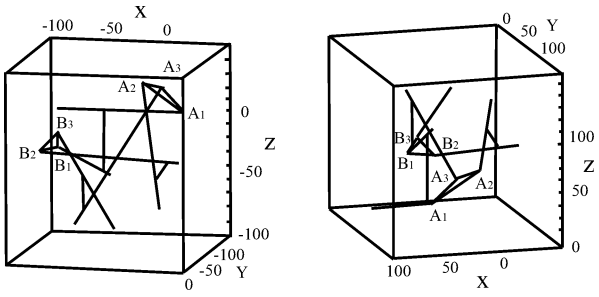

Fig. 5. The assembly configurations of two real solutions (root 7 and 8 in Table I).

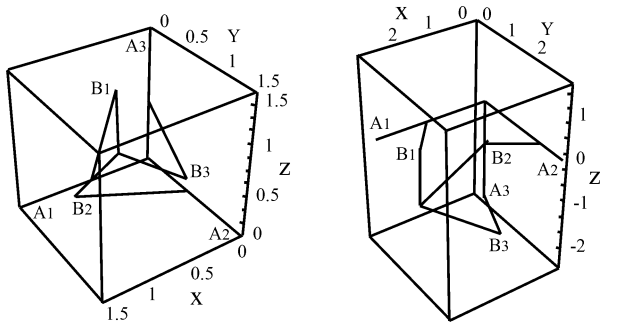

Fig. 6. The assembly configurations of two real solutions (root 6 and 8 in Table II).

$(1, 0, 0)$, $\boldsymbol{v}_2 = (0, 1, 0)$, $\boldsymbol{v}_3 = (0, 0, 1)$, $l_1 = l_2 = l_3 = 1.206$, $\alpha_1 = 60^\circ$, $\alpha_2 = 60^\circ$, $\alpha_3 = 60^\circ$. The solutions of the forward kinematics are obtained by using the procedure proposed above and listed in Table II. Two assembly configurations corresponding to two real solutions are shown in Fig. 6.

5. Comparison with the Traditional Stewart Platform

5.1. Kinematics

For the forward kinematics of the traditional Stewart–Gough platform, when Calay's formula is used to describe the orientation,[20] six equivalent polynomial equations are obtained from the original six geometrical constraint equations. After dealing with them with Gröbner basis theory, 18 basis equations are obtained and the problem of the forward displacement is reduced to a 40th degree polynomial equation in a single unknown from a constructed 13×13 Sylvester's matrix which is relatively small in the existing literatures Comparing with that, the process of solving the kinematics of the 3-CCC parallel mechanism leading to a 5×5 matrix in this paper is much simpler while the mechanism has the same mobility.

5.2. Workspace

Workspace is an important issue in the study of parallel mechanisms, which is usually investigated as reachable, constant-orientation[21] or orientation workspace. Several researchers addressed the determination of the workspace based on given leg length ranges.[22] This paper just gives

Table II. Solutions of example two.

	Solutions of orientation				Solutions of position corresponding to root 1 of orientation		
	c_1	c_2	c_3		x	y	z
1	$\sqrt{5}/5$	$\sqrt{5}/5$	$\sqrt{5}/5$	1	−1.70249	−0.411509	1.67734
2	$-\sqrt{5}/5$	$\sqrt{5}/5$	$\sqrt{5}/5$	2	−1.34567	2.03416	0.743181
3	$-\sqrt{5}/5$	$-\sqrt{5}/5$	$\sqrt{5}/5$	3	−0.768328	−0.768328	−0.768328
4	$-\sqrt{5}/5$	$-\sqrt{5}/5$	$-\sqrt{5}/5$	4	−0.411509	1.67734	−1.70249
5	$\sqrt{5}/5$	$-\sqrt{5}/5$	$\sqrt{5}/5$	5	0.743181	−1.34567	2.03416
6	$\sqrt{5}/5$	$\sqrt{5}/5$	$-\sqrt{5}/5$	6	1.1	1.1	1.1
7	$\sqrt{5}/5$	$-\sqrt{5}/5$	$-\sqrt{5}/5$	7	1.67734	−1.70249	−0.411509
8	$-\sqrt{5}/5$	$\sqrt{5}/5$	$-\sqrt{5}/5$	8	2.03416	0.743181	−1.34567

https://doi.org/10.1017/S0263574709990555 Published online by Cambridge University Press

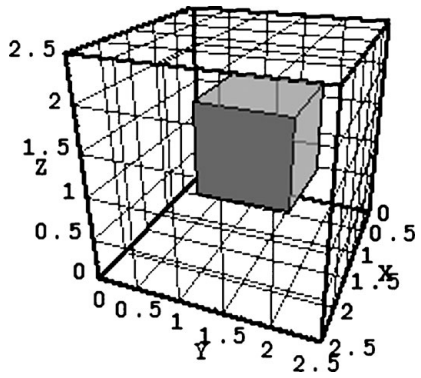

Fig. 7. Workspace of the 3CCC under a special orientation ($1 \leq l_i \leq 2$).

a short discussion by giving a special constant-orientation workspace of the new 3CCC parallel mechanism as in Fig. 1.

Workspace of a parallel mechanism usually depends on three parts except its mobility: limited link lengths, mechanical limits on the passive joints and links interference. For the 3CCC parallel mechanism, the limits of link lengths are $l_{\min} \leq l_i \leq l_{\max}$, $\alpha_{\min} \leq \alpha_i \leq \alpha_{\max}$, $(i = 1, 2, 3)$. As there are only cylindrical joints, the mechanical limits on the passive joints are the rotation angles (φ_i) of the cylindrical joints, which can be any amount of degree in the 3CCC parallel mechanism. Links interference follows Eq. (4) in literature.[23]

As the orientation and position of the moving platform of the 3CCC are decoupled, the limits of link lengths for the constant-orientation workspace will be $l_{\min} \leq l_i \leq l_{\max}$ only and α_i are known. Using the same parameters of example 2 in Section 4 and the constant orientation corresponding to solution 1 in Table II, the workspace can be given as shown in Figure 7.

From this case, we can find that the workspace under this orientation is simple and depend on the limits of the linkage lengths only. The traditional Stewart platform does not have this characteristic.

5.3. Control and trajectory planning

As studied in the kinematics, the orientation and position of the moving platform of the 3CCC are decoupled, the orientation depends on the angle constraints only, thus when we control the platform to a needed posture, there will be two steps:

(i) Firstly, plan the orientation by using Eq. (7) and the procedure in this paper to calculate the input (α_1, α_2, α_3) of the three limbs;
(ii) Secondly, consider the position by Eq. (8) to give the other three actuation (l_1, l_2, l_3) of the three limbs.

Thus it is much easier in control and trajectory planning of this new parallel mechanism comparing with the traditional Stewart platforms while their orientation and position are usually coupled and much more complex.

6. Conclusions

This paper presents the design of a CCC limb and a new 3CCC parallel mechanism. The screw analysis shows that this new limb does not constrain the moving platform and the 3CCC parallel mechanism has 6-DOF. The forward displacement analysis of a new 6-DOF 3CCC parallel mechanism, which has three distance constraints and three angle constraints between three pairs of lines in the base and platform. The forward positional equations are derived and the position and orientation are proved decoupled while both are of eighth order. The orientation is solved by reducing three angle constraint equations to a single eighth-order polynomial equation from a constructed 5×5 Dixon's matrix and the position is solved linearly. Two examples of application are reported which prove the efficiency of the process. The result of the 3CCC parallel mechanism is much easier than the general Stewart–Gough platform while they have the same mobility and the feature of decoupled orientation and position is also an advantage in trajectory planning. The workspace analysis proves special constant-orientation workspace and the traditional Stewart parallel mechanisms do not have this property. As the cylindrical joint is stiffer than the traditional spherical joint, the new design shown in this paper may be a better choice for the industry applications than the general Stewart ones when a full-DOF parallel mechanism is needed.

Acknowledgements

This work is partially supported by National Natural Science Foundation of China (50775012).

References

1. V. E. Gough, "Automobile Stability, Control, and Tyre Performance," *Proc. Automob. Div. Inst. Mech. Eng.* (1956) pp. 392–394.
2. D. Stewart, "A platform with six degree of freedom," *Proc. Inst. Mech. Eng. (Part I)* **180**(15), 371–386 (1965).
3. Q. Z. Liao, L. D. Senevirantne and S. W. E. Earles, "Forward Positional Analysis for the General 4–6 In-Parallel Platform," *Proc. Inst. Mech. Eng., C: J. Mech. Eng. Sci.* (1995) pp. 55–67.
4. O. Ma and J. Angeles, "Architecture Singularities of Platform Manipulators," *IEEE International Conference on Robotics and Automation*, Sacramento, CA (Apr. 1991) Vol. 2, pp. 1542–1548.
5. P. Cardou and J. Angeles, "Simplectic Architectures for True Multi-Axial Accelerometers: A Novel Application of Parallel Robots," *Proceedings of IEEE International Conference on Robotics and Automation*, Rome, Italy (Apr. 10–14, 2007) Vol. 110, pp. 181–186.
6. J. Merlet, "Direct kinematics of parallel manipulators," *IEEE Trans. Robot. Autom.* **9**, 842–846 (1993).
7. J. P. Merlet, Jacobian, "Manipulability, condition number, and accuracy of parallel robots," *ASME J. Mech. Des*. **128**, 199–206 (2006).
8. J. P. Merlet, "Dimensional Synthesis of Parallel Robots with a Guaranteed Given Accuracy Over a Specific Workspace," *Proceedings of IEEE International Conference on Robotics and Automation*, Barcelona, Spain (2005) pp. 942–947.
9. J. S. Dai, C. Sodhi and D. R. Kerr, "Design and Analysis of a New Six-Component Force Transducer Based on the Stewart Platform for Robotic Grasping," *Proceedings of the second Biennial European Joint Conference on Engineering Systems Design and* Analysis, London (July 4–7, 1994), ASME PD **64**(8–3), pp. 809–817 (1994).
10. K. Etemadizanganeh and J. Angeles, "Real-time direct kinematics of general 6-degree-of-freedom parallel manipulators

https://doi.org/10.1017/S0263574709990555 Published online by Cambridge University Press

with minimum-sensor data," *J. Robot. Syst.* **12**(12), 833–844 (1995).
11. M. L. Husty, "An algorithm for solving the direct kinematics of general Stewart–Gough platforms," *Mech. Mach. Theory* **31**, 365–380 (1996).
12. T.-Y. Lee and J.-K. Shim, "Improved dialytic elimination algorithm for the forward kinematics of the general Stewart–Gough platform," *Mech. Mach. Theorey* **38**, 563–577 (2003).
13. J. P. Merlet, "Solving the forward kinematics of a Gough-type parallel manipulator with interval analysis," *Int. J. Robot. Res.* **23**(3), 221–235 (2004).
14. X. S. Gao, D. Lei, Q. Liao and G. Zhang, "Generalized Stewart platforms and their direct kinematics," *IEEE Trans. Robot.* **21**, 141–151 (2005).
15. J. S. Dai and J. R. Jones, "Interrelationship between screw systems and corresponding reciprocal systems and applications," *Mech. Mach. Theory* **36**, 633–651 (2001).
16. J. Clark, *Robotics*, 3rd ed. (Mechanical Industry Press, Beijing, China, 2005).
17. O. Bottema and B. Roth, *Theoretical Kinematics* (North-Holland, New York, 1979) pp. 9–11.
18. B. R. Donald, D. Kapur and J. L. Mundy, *Symbolic and Numerical Computation for Artificial Intelligence* (Academic Press, London, 1992) pp. 52–55.
19. H. J. Su, Q. Z. Liao and C. G. Liang, "Direct positional analysis for a kind of 5–5 platform in-parallel robotic mechanism," *Mech. Mach. Theory* **34**, 285–301 (1999).
20. D. M. Gan, Q. Liao, J. Dai, S. Wei and L. Seneviratne, "Forward displacement analysis of the general 6–6 Stewart mechanism using Gröbner bases," *Mech. Mach. Theory* **44**, 1640–1647 (2009).
21. Qimi Jiang and C. M. Gosselin, "The maximal singularity-free workspace of the Gough–Stewart platform for a given orientation," *ASME J. Mech. Des.* **130**, 112304/1–8 (2008).
22. F. Pernkopf and M. Husty, "Workspace analysis of Stewart–Gough-type parallel manipulators," *Proc. Inst. Mech. Eng., Part C: J. Mech. Eng. Sci.* **220**(7), 1019–1032 (2006).
23. K. Y. Tsai and J. C. Lin, "Determining the compatible orientation workspace of Stewart–Gough parallel manipulators," *Mech. Mach. Theory* **41**, 1168–1184 (2006).

https://doi.org/10.1017/S0263574709990555 Published online by Cambridge University Press